

Polynomial expansion equalizers for communication via large antenna arrays

Ralf R. Müller
Forschungszentrum Telekommunikation Wien (FTW)
Vienna, Austria

Abstract

Polynomial expansion equalizers are found suitable to mitigate crosstalk and inter-symbol interference for communication via large antenna arrays. Design rules are derived from random matrix theory. The asymptotically optimum coefficients of the matrix polynomials are calculated analytically as a function of the number of receive antennas, transmit antennas, and scatterers for constant power delay profile. The theoretical results from random matrix theory are shown to accurately match data obtained by indoor measurements.

1 Introduction

Communication via antenna arrays allows for a significant increase in spectral efficiency [1, 2]. Several recent proposals [1, 3, 4, 5] are aiming to utilize this advantage in various ways. An inherent problem of these systems is distortion by crosstalk and inter-symbol interference arising from spatial and temporal multipath propagation.

The deleterious effects of crosstalk and inter-symbol interference can be mitigated by appropriate signal processing at receiver site if the correlation matrix of the channel is known or can be estimated accurately. Even suboptimum receivers that simply invert the channel or maximize the signal-to-interference-and-noise ratio (SINR) require to solve systems of linear equations that scale with the number of antenna elements. Therefore, it has been common belief that crosstalk and inter-symbol interference is the easier to combat the smaller the size of the arrays.

Mathematical results on the convergence of the eigenvalues of large dimensional random matrices yield a completely different view of the complexity of this problem. As the sizes of the channel matrices increase, the eigenvalues of the channels become more and more deterministic [6]. Since the quality of communication via linear vector channels is sufficiently determined by the eigenvalues of the channels' covariance matrices, the problem of efficient detection should simplify for systems with larger sizes, as they become more and more structured. This has been demonstrated successfully for interference mitigation in code-division

multiple-access (CDMA) in [7, 8, 9]. Indeed, this paper will show that efficient mitigation of crosstalk and inter-symbol interference is also feasible for communication via antenna arrays making use of recent results in [10, 11]. The complexity per bit of the proposed algorithm scales only linearly with the number of antenna elements.

2 Channel Model

Consider a communication link with T transmit and R receive antennas. Let there be S_{\max} scattering objects each corresponding to a propagation path with excess delay τ_κ . Then, the signal that is received at antenna ν is given by

$$y_\nu(t) = \sum_{\kappa=1}^{S_{\max}} A_\kappa e^{j\varphi_{\kappa,\nu}} \sum_{\mu=1}^T e^{j\vartheta_{\kappa,\mu}} x_\mu(t - \tau_\kappa) \quad (1)$$

where $x_\mu(t)$ is the signal transmitted at antenna μ and $\varphi_{\kappa,\nu}$, $\vartheta_{\kappa,\mu}$, and A_κ are the relative carrier phases at the ν^{th} receive and μ^{th} transmit antenna and the attenuation of the κ^{th} path, respectively. Note that each of the relative carrier phases depends on the distance between the individual antenna element and the scattering object.

Paths whose delays are not sufficiently separated in time cannot be resolved at the receiver. In order to model this effect all such paths are grouped in ascending order of their respective delays into L disjoint sets \mathcal{D}_ℓ such that all paths with similar delays form one

set. Then, the received signal at the ν^{th} antenna can be decomposed into

$$y_\nu(t) = \sum_{\ell=0}^{L-1} \sum_{\kappa \in \mathcal{D}_\ell} A_\kappa e^{j\varphi_{\kappa,\nu}} \sum_{\mu=1}^T e^{j\vartheta_{\kappa,\mu}} x_\mu(t - \tau_\kappa). \quad (2)$$

Thus, the propagation coefficient from antenna μ to antenna ν at the delay associated with index ℓ is given as

$$h_{\nu,\mu,\ell} = \sum_{\kappa \in \mathcal{D}_\ell} A_\kappa e^{j(\vartheta_{\kappa,\mu} + \varphi_{\kappa,\nu})}. \quad (3)$$

The number of scatterers may vary with delay. Therefore, it is sensible to model this effect by the scatterer-count delay profile¹ [10, 11]

$$S_\ell \triangleq |\mathcal{D}_\ell| \quad (4)$$

in addition to the well-known power-delay profile

$$P_\ell \triangleq \frac{1}{R} \sum_{\kappa \in \mathcal{D}_\ell} |A_\kappa|^2. \quad (5)$$

The received signal at fixed delay may be written in vector notation as

$$\mathbf{y}_\ell = \mathbf{H}_\ell \mathbf{x} \quad (6)$$

where the entries of the $R \times T$ matrix \mathbf{H}_ℓ are defined in (3). It is obvious from (3) that those entries show strong statistical dependencies even if A_κ , $e^{j\vartheta_{\kappa,\mu}}$, and $e^{j\varphi_{\kappa,\nu}}$ are statistically independent for all κ , μ , and ν . These dependencies are examined in greater detail in the following.

Assume without loss of generality that $\mathcal{D}_\ell = \{1, 2, \dots, S_\ell\}$. Define the two $S_\ell \times T$ and $S_\ell \times R$ matrices

$$\mathbf{\Theta}_\ell \triangleq \begin{bmatrix} e^{j\vartheta_{1,1}} & \dots & e^{j\vartheta_{1,T}} \\ \vdots & \ddots & \vdots \\ e^{j\vartheta_{S_\ell,1}} & \dots & e^{j\vartheta_{S_\ell,T}} \end{bmatrix} \quad (7)$$

and

$$\mathbf{\Phi}_\ell \triangleq \begin{bmatrix} e^{-j\varphi_{1,1}} & \dots & e^{-j\varphi_{1,R}} \\ \vdots & \ddots & \vdots \\ e^{-j\varphi_{S_\ell,1}} & \dots & e^{-j\varphi_{S_\ell,R}} \end{bmatrix}, \quad (8)$$

respectively, as well as $\mathbf{A}_\ell \triangleq \text{diag}([A_1, \dots, A_{S_\ell}])$. Then, \mathbf{H}_ℓ may be expressed as

$$\mathbf{H}_\ell = \mathbf{\Phi}_\ell^H \mathbf{A}_\ell \mathbf{\Theta}_\ell \quad (9)$$

with \cdot^H denoting the Hermite operator. If there is no line of sight and the antennas within the transmitter array are spaced sufficiently far apart from each other, it is reasonable to assume that the entries within the

matrices $\mathbf{\Theta}_\ell$ are statistically independent. A corresponding statement holds for the receiver array and the matrices $\mathbf{\Phi}_\ell$.

It is not obvious whether the two matrices $\mathbf{\Theta}_\ell$ and $\mathbf{\Phi}_\ell$ are mutually statistically independent, in practice. In particular, strong dependencies are implied by the single scattering model [12]. In contrast, physical measurements indicate that the correlations between the direction of arrival and the direction of departure are not significant [13, 14]. This supports the proposal that statistical independence of $\mathbf{\Theta}_\ell$ and $\mathbf{\Phi}_\ell$ is realistic. For the following calculations, independence is assumed. Anyhow, the accuracy of the proposed model for the design of polynomial expansion equalizers is confirmed by measurements in Section 5.

3 Proposed Receiver Design

For ease of notation, we first consider the case without inter-symbol interference, i.e. $L = 1$, and drop the index ℓ . Later on our results are generalized to arbitrary L .

A receiver that aims to maximize the SINR in presence of additive white Gaussian noise (AWGN) of variance $\sigma^2 P$ needs to calculate the estimate

$$\left(\mathbf{H}^H \mathbf{H} + \sigma^2 \mathbf{I} \right)^{-1} \mathbf{H}^H \mathbf{y}. \quad (10)$$

The detector in (10) involves the inversion of a matrix. This is a hard task for real-time applications, but can be approximated very efficiently for large number of antennas as shown in the following.

The Cayley-Hamilton theorem states that any matrix is a zero of its characteristic polynomial, i.e.

$$\prod_{i=1}^T \left(\mathbf{H}^H \mathbf{H} + \sigma^2 \mathbf{I} - (\lambda_i + \sigma^2) \mathbf{I} \right) = \mathbf{0} \quad (11)$$

with λ_i , $1 \leq i \leq T$ denoting the eigenvalues of $\mathbf{H}^H \mathbf{H}$. The polynomial can be written also as

$$\sum_{i=0}^T \alpha_i (\lambda_1, \dots, \lambda_T; \sigma^2) \left(\mathbf{H}^H \mathbf{H} + \sigma^2 \mathbf{I} \right)^i = \mathbf{0} \quad (12)$$

with appropriate coefficients α_i depending on the eigenvalues of \mathbf{C} and the variance of the AWGN. We can rewrite (12) into

$$\left(\mathbf{H}^H \mathbf{H} + \sigma^2 \mathbf{I} \right)^{-1} = - \sum_{i=0}^{T-1} \frac{\alpha_{i+1}}{\alpha_0} \left(\mathbf{H}^H \mathbf{H} + \sigma^2 \mathbf{I} \right)^i \quad (13)$$

and obtain the inverse in (10) as a matrix polynomial of degree $T - 1$ with coefficients depending on the eigenvalues and the noise variance only.

¹ $|\cdot|$ denotes the cardinality of a set.

$$\begin{aligned}
m_1 &= (m_2 + \sigma^2 m_1)w_0 & + & (m_3 + \sigma^2 m_2)w_1 & + \dots + & (m_{D+2} + \sigma^2 m_{D+1})w_D \\
m_2 &= (m_3 + \sigma^2 m_2)w_0 & + & (m_4 + \sigma^2 m_3)w_1 & + \dots + & (m_{D+3} + \sigma^2 m_{D+2})w_D \\
\vdots & & & \vdots & & \ddots & \vdots \\
m_{D+1} &= (m_{D+2} + \sigma^2 m_{D+1})w_0 & + & (m_{D+3} + \sigma^2 m_{D+2})w_1 & + \dots + & (m_{2D+2} + \sigma^2 m_{2D+1})w_D
\end{aligned} \tag{15}$$

Random matrix theory [15] shows that the eigenvalue distributions of a large class of random matrices converge in probability to some deterministic limits if the sizes of the matrices grow over all bounds. The limiting statistics of \mathbf{H} have been calculated in [10, 11]. Since the eigenvalues converge to a deterministic limit for large matrices, so the coefficients of the polynomial in (13) do. Thus, the coefficients do not depend on the actual realization of the matrix \mathbf{H} as the number of antennas grows large. Therefore, there is no need to calculate them in real-time via eigenvalue decomposition of $\mathbf{H}^H \mathbf{H}$ (or singular value decomposition of \mathbf{H}) when the channel is fading.

For practical purposes, (13) might still be too complex as the number of transmit antennas T was assumed to be large. Now, we ask for the optimum coefficients w_i such that the polynomial

$$\sum_{i=0}^D w_i \left(\mathbf{H}^H \mathbf{H} + \sigma^2 \mathbf{I} \right)^i \tag{14}$$

is the best approximation to the inverse in (10) for a given degree D that is smaller than $T - 1$.

Defining optimality in the sense that the SINR after equalization with the approximate inverse is maximum has been addressed in [8, 16]: In the case of asymptotically large covariance matrices, the optimum weights were shown to be the solution to a system of Yule-Walker equations (15) depending on the moments of the asymptotic eigenvalue distribution $m_k, 1 \leq k \leq 2D + 2$ and the noise variance.

For communication via antenna arrays with equal attenuation on each propagation path, the moments for $n > 0$ are given in [10, 11] as

$$m_n = P^n \sum_{i=0}^{n-1} \sum_{j=0}^{n-1} \binom{n}{i} \binom{n}{j} \binom{n}{i+j+1} \frac{\beta^i \zeta^j}{n} \tag{16}$$

with the parameters

$$\beta \triangleq \frac{T}{R} \quad \text{and} \quad \zeta \triangleq \frac{T}{S} \tag{17}$$

called *system load* and *channel load*. In that case, the solutions to (15) for $D = 1$ and $D = 2$ read

$$\begin{aligned}
w_1 &= -\beta\zeta - \beta - \zeta \\
w_0 &= -(\sigma^2/P + 2 + 2\beta + 2\zeta)w_1 + \beta\zeta
\end{aligned} \tag{18}$$

and

$$\begin{aligned}
w_2 &= \beta^3 \zeta^3 + 3\beta^3 \zeta + 3\beta^2 \zeta + 3\beta \zeta^3 + 3\beta \zeta^2 \\
&\quad + 5\beta^2 \zeta^2 + 3\beta^3 \zeta^2 + 3\beta^2 \zeta^3 + \zeta^3 + \beta^3 \\
w_1 &= -\left(\frac{\sigma^2}{P} + 3 + 3\beta + 3\zeta\right)w_2 - 2\beta^3 \zeta - 4\beta^2 \zeta^2 \\
&\quad - 2\beta \zeta^3 - 4\beta^3 \zeta^2 - 4\beta^2 \zeta^3 - 2\beta^3 \zeta^3 \\
w_0 &= -\frac{\sigma^2}{P} w_1 + (3 + 5\beta + 5\zeta + 5\beta \zeta + 3\beta^2 + 3\zeta^2)w_2 \\
&\quad + 2\beta^2 \zeta^2 + 2\beta^4 \zeta^2 + 2\beta^2 \zeta^4 + 11\beta^3 \zeta^3 \\
&\quad + 11\beta^3 \zeta^2 + 11\beta^2 \zeta^3 - \beta^4 - \zeta^4 - \beta^4 \zeta^4
\end{aligned} \tag{19}$$

respectively. Solutions for $D > 2$ are not listed here. They can be obtained with symbolic algebra software from (15) and (16).

The direct implementation of the matrix polynomial is not the most efficient one. In CDMA communications, i.e. $\zeta = 0$, it is advantageous to implement the matrix polynomial by subsequent re-spreading and matched-filtering blocks whose outputs are combined with the appropriate weights $w_i, 0 < i < D$, see [17]. This method avoids matrix multiplications and makes the complexity per bit scale only linearly with the size of the matrices involved in the calculations. For $D = 1$, the method in [17] can be generalized to work in combination with successive decoding [8, 16]. The approaches reported in [17, 8, 16] have direct counterparts in antenna array communications: The spreading sequences and the number of users correspond to the columns of the channel matrix \mathbf{H} and to the number of transmit antennas T , respectively. As an additional parameter the channel load ζ enters the weight design. Therefore, no matrix inversions or eigenvalue decompositions are required to compute a near-optimum linear beam former at receiver site in real-time. Only accurate estimates of the channel matrix \mathbf{H} and the channel load ζ are essential.

4 Inter-Symbol Interference

Previously, inter-symbol interference has been neglected. Inter-symbol interference can be described in matrix algebra by a space-time channel matrix as in (20), see top of next page, where the matrix-valued symbols $\mathbf{x}[k]$ and $\mathbf{y}[k]$ at transmitter and receiver site, respectively, that are sent at subsequent time instances k are stacked into a single vector each.

Surprisingly, it can be shown [10, 11] that the asymptotic eigenvalue distribution of the space-time

$$\begin{bmatrix} \vdots \\ \mathbf{y}[0] \\ \mathbf{y}[1] \\ \mathbf{y}[2] \\ \vdots \end{bmatrix} = \underbrace{\begin{bmatrix} \ddots & \ddots & \ddots & \ddots & \ddots & \ddots & \ddots & \ddots & \ddots & \ddots \\ \cdots & \mathbf{0} & \mathbf{H}_{L-1} & \cdots & \mathbf{H}_1 & \mathbf{H}_0 & \mathbf{0} & \cdots & \cdots & \cdots \\ \cdots & \cdots & \mathbf{0} & \mathbf{H}_{L-1} & \cdots & \mathbf{H}_1 & \mathbf{H}_0 & \mathbf{0} & \cdots & \cdots \\ \cdots & \cdots & \cdots & \mathbf{0} & \mathbf{H}_{L-1} & \cdots & \mathbf{H}_1 & \mathbf{H}_0 & \mathbf{0} & \cdots \\ \cdots & \cdots & \cdots & \cdots & \ddots & \ddots & \ddots & \ddots & \ddots & \ddots \end{bmatrix}}_{\triangleq \mathcal{H}} \begin{bmatrix} \vdots \\ \mathbf{x}[0] \\ \mathbf{x}[1] \\ \mathbf{x}[2] \\ \vdots \end{bmatrix} \quad (20)$$

channel matrix \mathcal{H} is identical to those one of

$$\sum_{\ell=0}^{L-1} \mathbf{H}_{\ell}. \quad (21)$$

Under the additional assumption of constant power delay profile, its moments are also given by (16) [10, 11] with channel load

$$\zeta \triangleq \frac{T}{S_{\max}}. \quad (22)$$

Therefore, at least for constant power delay profile, one can apply the same structure for space-time equalization as proposed in the previous section for solely spatial equalization. Moreover, Section 5 will show that the deviations from (16) caused by realistic power delay profiles are moderate.

5 Comparison to Measurements

Previously, several assumptions, i.e. asymptotically large arrays, constant power delay profile, statistical independence among the entries of Φ and Θ , etc., have been made. The motivation behind these assumptions was analytical tractability. Moments calculated under such idealized assumptions are not sure to adequately match eigenvalue statistics experienced in practice. This section provides a comparison between the moments of the eigenvalue distributions of space-time channels matrices calculated from the channel model proposed in Section 2 to those ones observed in an indoor measurement campaign with the vector channel sounder RUSK-ATM manufactured by Medav GmbH.

All measurements mentioned in the following were recorded with a bandwidth of 120 MHz around a carrier frequency of 2 GHz. The receiver was an 8-element linear patch array spaced at half a wavelength. The transmitter was a single omni-directional dipole antenna that was re-located by software control over a straight line in steps of half a wavelength. The patch array was directed in such a way that line-of-sight was blocked.

The raw data provided by the vector channel sounder RUSK-ATM are matrix-valued complex frequency responses of the antenna array channel. Since

the design parameters for polynomial expansion equalizers are the moments of the eigenvalue distributions of the channels' space-time covariance matrices, the latter were extracted from the raw measurement data. Following the reasoning in [10, 11], see also in the appendix, this can be achieved by

$$\hat{m}_n = \frac{\int_{1.94 \text{ GHz}}^{2.06 \text{ GHz}} \text{trace} \left(\mathbf{H}^H(f) \mathbf{H}(f) \right)^n df}{\int_{1.94 \text{ GHz}}^{2.06 \text{ GHz}} \text{trace} \left(\mathbf{H}^H(f) \mathbf{H}(f) \right) df} \quad (23)$$

where $\mathbf{H}(f)$ and \hat{m}_n denote the matrix-valued frequency response and the measured n^{th} moment, respectively.

For the first measurement described in this paper, the receiver was located in the author's office while the transmitter was placed in an adjacent room. The moments of the eigenvalue distribution obtained from this measurement via (23) are given in the first row of Table 1. For comparison, the moments calculated under the assumption of $S_{\max} = 6$ scattering objects of unit power using (16) are given in the second row of Table 1. The accurate fit of the calculated and measured moments give rise to the assumption that there actually happened to be 6 dominant scattering objects.

In order to investigate the influence of the number of scattering objects, we stucked scrambled tin foil, 35 pieces altogether and each about 1 m² in size, onto the walls, floors, ceilings, and furniture close to either receiver or transmitter. The moments measured from the same antenna positions with the help of tin foil are given in the third row of Table 1. They accurately match those moments calculated from (16) under the assumption of $S_{\max} = 30$ scattering objects of unit power, cf. fourth row in Table 1. For comparison, the fifth row of Table 1 shows the moments calculated from the probability density function of the eigenvalues of a covariance matrix that results from an 8 × 8 channel matrix with independent complex Gaussian entries reported in [18]. Although reference [18] accounts for the finite size of the antenna array while the author's model [10, 11] uses matrices of infinite size, the as-

$R = T = 8$	$\bar{\lambda}$	$\bar{\lambda}^2$	$\bar{\lambda}^3$	$\bar{\lambda}^4$	$\bar{\lambda}^5$	$\bar{\lambda}^6$	$\bar{\lambda}^7$	$\bar{\lambda}^8$
measured without tin foil	1.00	3.32	14.66	74.17	406.25	2344.80	14044.97	86485.64
calculated for $\zeta = 8/6$	1.00	3.33	14.78	75.04	412.57	2390.29	14371.71	88832.83
measured with tin foil	1.00	2.34	6.96	23.03	81.37	301.13	1155.06	4560.53
calculated for $\zeta = 8/30$	1.00	2.27	6.67	22.34	80.78	307.44	1213.28	4920.13
i.i.d. [18]	1.00	2.00	5.02	14.16	43.10	138.60	465.61	1622.79

Table 1: Moments of eigenvalue distributions. Measured in the author’s office without tin foil, calculated for $S_{\max} = 6$, measured with tin foil, calculated for $S_{\max} = 30$, and under i.i.d. assumption, resp.

sumption of independent identically distributed (i.i.d.) entries which corresponds to infinitely rich scattering drives the model far apart from the measured situations.

The close fit between the theoretical predictions and the actual measurements in Table 1 are both a convincing confirmation for the random matrix model for antenna array channels introduced in [10, 11] and for the applicability of (16) for design of polynomial expansion equalizers.

Limitations of the equal power assumption:

The moments calculated by (16) refer to equal path loss for any scattering object. This assumption is well justified for an almost constant power delay profile. It is also justified as long as the number of dominant scattering objects is not much smaller than the number of antenna elements on either side. The latter condition is not straightforward. Therefore, it is explained in greater detail in the following: There are not more non-zero eigenvalues than $\min\{R, T\}$. Thus, only the $\min\{R, T\}$ most powerful scatterers show significant influence onto the eigenvalue distribution. Note that for higher order moments the power imbalances are more and more amplified.

In order to give a fair comparison, moments of eigenvalue distributions of channel covariance matrices are measured under propagation conditions which do not allow for negligence of power imbalances. Such a situation was found in a large factory hall (about 120 m \times 120 m) where the larger delays created the power delay profile shown in Fig. 1. The moments measured in the factory hall are shown in the first row of Table 2. The second row of Table 2 shows the moments calculated via (16) for $S_{\max} = 3$ unit power scatterers which turned out to fit best to the measured data. It can be observed that the fit is not as good as in Table 1, but by far better than with the i.i.d. assumption. Note also that the relative deviation is largest for the lower order moments². For those ones, the measured values are lower indicating more than 3 scatterers. Since these additional scatterers are received less powerful, their influence vanishes more and more at higher order moments.

²Note that the first moment was normalized to 1.

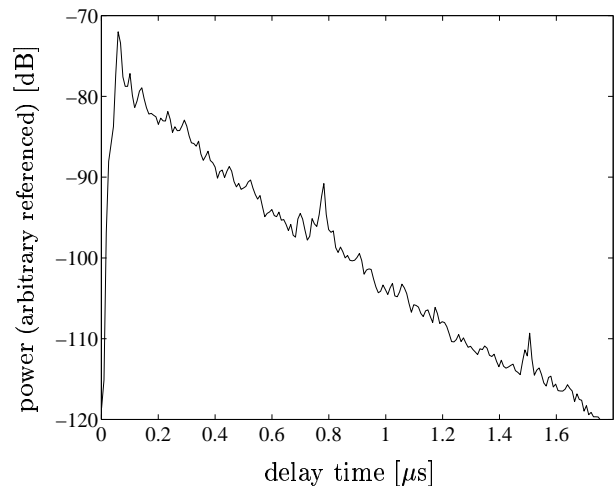


Figure 1: Power delay profile in factory hall averaged over all antenna elements.

6 Conclusions

Space-time equalizers for communication via large antenna arrays have been proposed. Convergence theorems from random matrix theory have been the key tool to find solutions to large systems of linear equations easily. The proposed method originally suggested for detection of CDMA has turned out to be even more advantageous for antenna array channels where it has also capabilities to combat inter-symbol interference. In addition, a new method for equalization of inter-symbol interference on antenna array channels has been found that results from random matrix theory and does not exist on channels without multiple inputs/outputs at both ends of the communication link. The theoretical predictions derived from random matrix theory in [10, 11] have been shown to accurately match measurement data.

Using random matrix theory for both the channel model and the receiver design, joint equalization of inter-symbol interference and crosstalk becomes an easy task for large antenna arrays if accurate channel estimates are available.

$R = 8, T = 15$	$\bar{\lambda}$	$\bar{\lambda}^2$	$\bar{\lambda}^3$	$\bar{\lambda}^4$	$\bar{\lambda}^5$	$\bar{\lambda}^6$	$\bar{\lambda}^7$	$\bar{\lambda}^8$
measured	1.00	6.42	61.30	697.39	8881.86	123274.77	1830529.35	28643903.66
calculated	1.00	7.88	78.27	881.65	10715.90	137017.99	1816515.49	24744069.10
i.i.d. [18]	1.00	2.87	10.16	40.16	170.57	762.02	3538.39	16954.77

Table 2: Moments of eigenvalue distributions. Measured in a factory hall, calculated for $S_{\max} = 3$, and under i.i.d. assumption, resp.

Acknowledgment

The author would like to thank S. Verdú, C. Mecklenbräuker, and K. Kopsa for helpful discussions, H. Hofstetter, H. Kunczier, and M. Lončar who carried out the measurements, Siemens AG, Austria, for providing access to one of their factory halls, and T-Nova Deutsche Telekom Innovationsgesellschaft bmH for borrowing the 8-element array antenna.

Appendix

The purpose of this appendix is to confirm (23). Although it straightforwardly follows from the considerations in [11, 10], here a short motivation is given for sake of completeness.

The goal of (23) is to calculate the moments of the eigenvalue distribution of the space-time covariance matrix $\mathcal{H}^H \mathcal{H}$ where \mathcal{H} is defined in (20). Since the channel sounder RUSK-ATM does not measure the matrix-valued impulse response $\mathbf{H}_\ell, 0 \leq \ell \leq L-1$, but the matrix-valued transfer function $\mathbf{H}(f)$ at many samples of the frequency range, an appropriate method for calculating the moments is needed.

One of such methods is certainly to perform RT -inverse fast Fourier transforms (IFFTs) in parallel over the transfer functions $\mathbf{H}_{ij}(f), 1 \leq i \leq R, 1 \leq j \leq T$, compose the space-time channel matrix \mathcal{H} , and then calculate the moments of $\mathcal{H}^H \mathcal{H}$. However, that method is both computationally heavy and inaccurate, since it requires windowed IFFTs. An easier and more accurate method is as follows: Note that \mathcal{H} is a circulant matrix, cf. (20), since its rows and columns are filled up towards both ends with infinitely many (matrix-valued) zero elements. Therefore, the space-time covariance matrix can be decomposed into

$$\mathcal{H}^H \mathcal{H} = \mathcal{T} \mathcal{L} \mathcal{T}^H$$

where \mathcal{L} is a block-diagonal matrix, and \mathcal{T} is a Fourier matrix on the set of $T \times T$ identity matrices, i.e. \mathcal{T} is the Kronecker product of a Fourier matrix with a $T \times T$ identity matrix. Since \mathcal{T} is unitary, the moments of the space-time covariance matrix are identical to those ones of \mathcal{L} . Note that \mathcal{L} is block-diagonal and the $T \times T$ blocks are composed from the frequency responses $\mathbf{H}(f)^H \mathbf{H}(f)$ at all frequency samples within

the range of the measurement. Therefore, calculating the moments of the space-time covariance matrix is equivalent to averaging the moments of the matrix-valued frequency response over all frequencies as done in (23).

References

- [1] G. J. Foschini. Layered space-time architecture for wireless communication in a fading environment when using multi-element antennas. *Bell Labs Technical Journal*, 1(2):41–59, 1996.
- [2] G. Foschini and M. Gans. On limits of wireless communications in a fading environment when using multiple antennas. *Wireless Personal Communications*, 6:311–335, 1998.
- [3] G. G. Raleigh and J. M. Cioffi. Spatio-temporal coding for wireless communication. *IEEE Transactions on Communications*, 46(3):357–366, Mar. 1998.
- [4] V. Tarokh, N. Seshadri, and A. R. Calderbank. Space-time codes for high data rate wireless communications: Performance criterion and code construction. *IEEE Transactions on Information Theory*, 44(2):744–765, Mar. 1998.
- [5] H. Bölcskei, D. Gesbert, and A. J. Paulraj. On the capacity of wireless systems employing OFDM-based spatial multiplexing. *Submitted to IEEE Transactions on Communications*, Oct. 1999.
- [6] V. A. Marcenko and L. A. Pastur. Distribution of eigenvalues for some sets of random matrices. *Math. USSR-Sb*, (1):457–483, 1967.
- [7] D. Guo, L. K. Rasmussen, and T. J. Lim. Linear parallel interference cancellation in long-code CDMA multiuser detection. *IEEE Journal on Selected Areas in Communications*, 17(12):2074–2081, Dec. 1999.
- [8] R. R. Müller. Approximate MMSE multiuser detection. Technical report, German Academic Exchange Service, Bonn, Germany, Apr. 2000.

- [9] R. R. Müller and S. Verdú. Design and analysis of low-complexity interference mitigation for CDMA. In *COST 262 Workshop on Multiuser Detection in Spread Spectrum Communications*, Ulm, Germany, Jan. 2001.
- [10] R. R. Müller. A random matrix model of communication through antenna arrays. In *Proc. of 38th Annual Allerton Conference on Communications, Control and Computing*, Monticello, IL, U.S.A. Oct. 2000.
- [11] R. R. Müller. A random matrix theory of communication via antenna arrays. *Submitted to IEEE Transactions on Information Theory*, Aug. 2000.
- [12] J. C. Liberti jr. and T. S. Rappaport. *Smart Antennas for Wireless Communications*. Prentice-Hall, 1999.
- [13] M. Steinbauer, D. Hampicke, G. Sommerkorn, A. Schneider, A. F. Molisch, R. Thomä, and E. Bonek. Array measurement of the double-directional mobile radio channel. In *Proc. of IEEE Vehicular Technology Conference*, Tokio, Japan, May 2000.
- [14] M. Steinbauer, A. F. Molisch, and E. Bonek. The double-directional mobile radio channel. *Submitted to IEEE Antennas and Propagation Magazine*, Aug. 2000.
- [15] D. V. Voiculescu, K. J. Dykema, and A. Nica. *Free Random Variables*. American Mathematical Society, Providence, RI, 1992.
- [16] R. R. Müller and S. Verdú. Design and analysis of low-complexity interference mitigation on vector channels. *Submitted to IEEE Journal on Selected Areas in Communications*, Dec. 2000.
- [17] E. Kanterakis and S. Moshavi. Multistage linear receiver for DS-CDMA systems, May 1998. US-patent US5757791.
- [18] I. E. Telatar. Capacity of multi-antenna Gaussian channels. *European Transactions on Telecommunications*, 10(6), Nov/Dec. 1999.